Digital Object Identifier: 10.1109/ULTSYM.2008.0168

Internal Phase Inversion Narrow Bandwidth MEMS Filter

Jize Yan, Ashwin A. Seshia
Department of Engineering
University of Cambridge
Cambridge, United Kingdom
Email: jy242@cam.ac.uk

Kim Le Phan, Joost T.M. van Beek
NXP Semiconductors
Philips Campus
5656AA Eindhoven
The Netherlands

***Abstract*—This paper reports a novel capacitively coupled twin beam resonator internal phase inversion filter fabricated in a SOI MEMS process. A narrow bandwidth of 0.0157% is demonstrated with a low control-voltage of -0.87V. The bandwidth can be substantially reduced by utilizing an electrical coupling spring as opposed to a mechanical coupling-spring. The bandwidth is tunable with control achieved using a differential DC bias. A summary and comparison with other members of the phase inversion filter family is also included.**

Keywords-MEMS, resonators, filters, narrow bandwidth

I. INTRODUCTION

There is much interest in the development of MEMS-based voltage-controlled and highly-selective bandpass filters. We have recently reported electrical [1] and mechanical [2] phase inversion in coupled MEMS resonator arrays as a solution towards overcoming the effects of capacitive parasitics intrinsic to many microfabrication processes. However, achieving narrow bandwidth utilising mechanically coupled resonator arrays is challenging at very high frequencies in part due to the practical limitations in coupling very tiny electro-mechanical signals between the resonators. Previous solutions [3][4] are often restricted by the requirement for high DC voltages that can run counter to the miniaturization and integration trends of RF front ends.

In this paper, we demonstrate a novel MEMS filter with a narrow bandwidth (0.0157%) and a low control-voltage (< -1V). A novel capacitive coupling method is utilized in a twin beam resonator-array, which can substantially reduce the bandwidth compared with mechanical-coupling. Internal phase inversion with differential DC-bias driving [1] is utilized to realize filter performance. Section II describes device modeling and characterization. Section III summarizes the coupling methods utilized in the phase inversion MEMS filters family.

II. DEVICE MODELING AND CHARACTERIZATION

A. Device

The filter consists of two free-free beam resonators anchored at the nodal points as shown in Fig. 1. The two beam resonators are capacitively coupled by the transduction gap between each other and driven synchronously by the input ports indicated in Fig. 1. The right and left beam resonators are connected to the output port and ground port, respectively. Different DC-bias is applied on the input and output ports.

This work was supported by the EU FP 6 Project NANOTIMER.

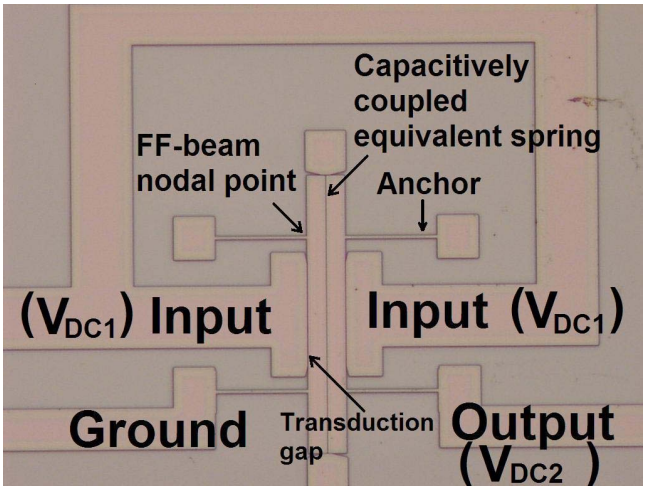

Figure 1. Optical micrograph of the fabricated SOI MEMS filter.

B. Transduction Mechanism

Fig. 2 shows a schematic layout of the equivalent transduction mechanism. The twin-beam resonator-array filter is a combination of two resonators, one with two transduction gaps (left) and the other with a single transduction gap only (right).

The small-signal (linear) equivalent electrical circuit for a resonator with one transduction gap is shown in Fig. 3 (a) [1][7], where *Rm*, *Cm* and *Lm* represent the motional resistance, motional capacitance and motional inductance, respectively.

The resonator with two transduction gaps utilises an input port for driving and an output port for sensing. The small-signal equivalent circuit is shown in Fig. 3 (b). As the two ports are on the opposite side of the resonator, the change in capacitance nominally satisfies

$$\frac{\partial C_1}{\partial x} = -\frac{\partial C_2}{\partial x} \quad (1)$$

The transduction coefficients at the input port and output port are defined as $\eta_1=V_{P1}(\partial C_1/\partial x)$ and $\eta_2=V_{P2}(\partial C_2/\partial x)$, respectively [7]. When DC-bias is applied to the two ports, the relation of the transduction coefficients can be expressed as

$$\eta_1 = \begin{cases} -\eta_2 & if\ V_{DC-input} = V_{DC-output} \\ \eta_2 & if\ V_{DC-input} = -V_{DC-output} \end{cases} \quad (2)$$

The transduction gain of the output port is given by

$$\phi = \frac{\eta_2}{\eta_1} = \begin{cases} -1 & if\ V_{DC-input} = V_{DC-output} \\ 1 & if\ V_{DC-input} = -V_{DC-output} \end{cases} \quad (3)$$

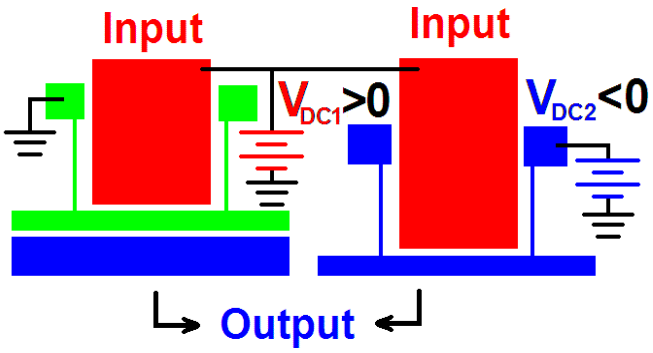

Figure 2. Equivalent transduction mechanism for the twin-beam resonator

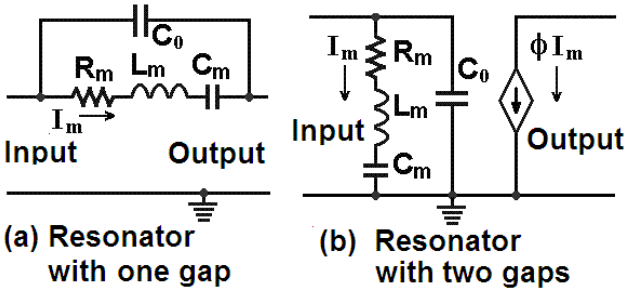

Figure 3. Equivalent electrical circuits for the twin-beam resonators.

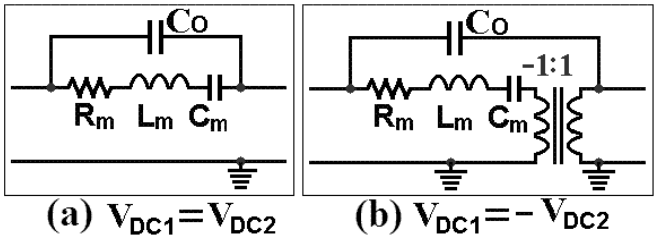

Figure 4. Equivalent electrical circuits for one of the twin-beam resonators with two tranducation gaps.

When driving each resonator independently utilizing in-phase or differential DC bias, the circuits can be further simplified as shown in Fig. 4 [8]. Fig. 4(a) represents the circuit with in-phase DC-bias ($V_{DC1}=V_{DC2}$, $\Phi=-1$), while Fig. 4(b) describes the circuits with differential DC-bias ($V_{DC1}=-V_{DC2}$, $\Phi=1$). Co is the series (feedthrough) capacitance of the resonator. The relative phase shift between the motional and feedthrough currents in the two cases shown in Figs. 4 (a) and (b) is 180°. The 180° phase shift induces the frequency of the anti-resonance (parallel resonance) to be lower than the series resonant frequency with differential DC-bias, while the reverse is true with in-phase DC-bias.

The effects of the feedthrough capacitance on series and parallel resonance is illustrated using a clamped-clamed beam resonator fabricated in the same process. The results from experimental characterisation are shown in Fig. 5. The relation between anti-resonance and series-resonance with in-phase or differential DC-bias is as predicted.

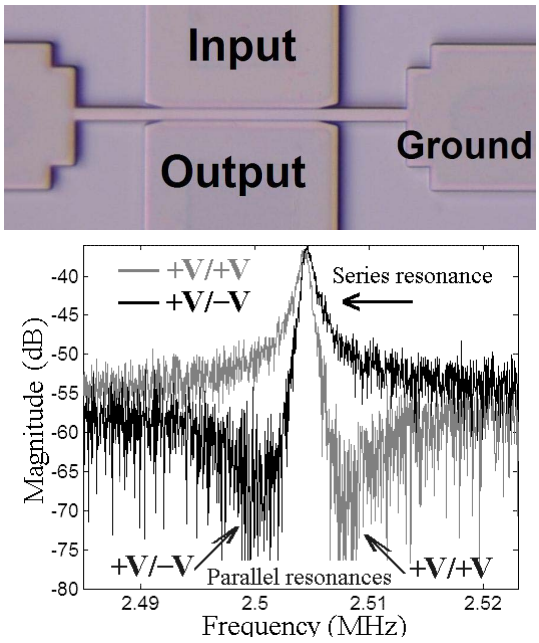

Figure 5. Clamped-clamped beam resonator, and its magnitude of S-parameters measurements with in-phase or differential DC-bias

Thus the combined equivalent electrical circuit for the twin-beam resonator array filter with in-phase or differential DC-bias can be established as shown in Fig. 6.

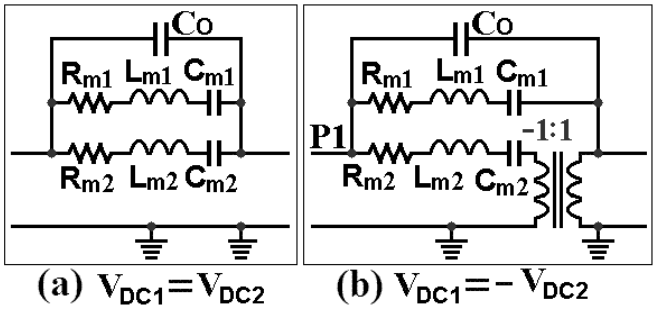

Figure 6. Electrical equivalent circuits of twin-beam resonator arrays with in-phase or differential DC-bias

C. *Minimum Filter Bandwidth*

The finite element analysis (FEA) simulation results of the in-phase and out-of-phase modes of the twin-beam filter

are shown in Fig. 7. The out-of-phase mode is due to the middle capacitively coupled transduction gap, which works as a coupling spring and the discrete lumped mechanical model is illustrated in Fig. 8, wherein k_C is the coupling spring, k and m are the effective spring constant and equivalent mass of the FF-beam resonators, respectively.

The natural frequencies for two modes can be obtained from the vibration constitution equation $|\boldsymbol{K}-\omega^2\boldsymbol{M}|=\boldsymbol{0}$ [5] which gives the following solution

$$\omega^2 = \frac{k_1 + k_2 + 2k_C \pm \sqrt{(k_1 - k_2)^2 + 4k_C^2}}{2m} \quad (4)$$

$$\omega_{out}^2 - \omega_{in}^2 = \sqrt{(k_1 - k_2)^2 + 4k_C^2}\,/m \quad (5)$$

The minimum difference between the two frequencies is determined as

$$\omega_{out}^2 - \omega_{in}^2 \geq |2k_C|/m \quad (6)$$

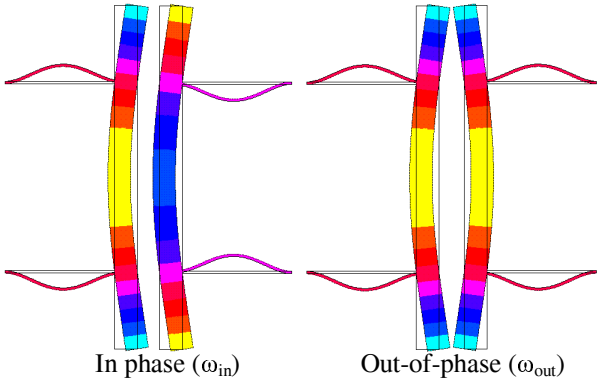

Figure 7. FEA simulation of the twin-beam resonator filter

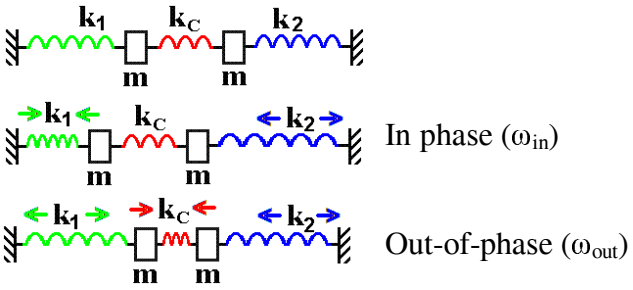

Figure 8. Schematic of a spring coupled mechanical filter

In the current work, the coupling spring k_C is an electrical spring [6]. An expression for the electrical spring can be written as

$$k_C = C_0 V_P^2 / g^2 \quad (7)$$

where C_0 is the transduction capacitance, g is the transduction gap, V_P is the DC driving voltage between the gap that is equal to the output port control voltage V_{DC2} as shown in Fig. 7.

By reducing the transduction DC driving voltage, the electrical equivalent spring k_C can be made very small, an order of magnitude or less than mechanical springs that are limited by fabrication tolerances. Thus, capacitive-coupling can be utilised to introduce weak coupling between resonant systems and tailor the filter bandwidth precisely.

D. Device Operation and Filter Performance

As derived in Eq. (7), the output port DC-bias V_{DC2} controls the capacitively coupled equivalent spring. After applying a DC-bias on the input port of the MEMS resonator, a small negative control voltage is applied on the output port to induce an inverse phase current (differential DC-bias driving), which can be coupled with the motional current to construct filter performance as shown in the in Fig. 9 (see blue dotted curve), with a frequency of 4.134MHz, a 3dB-bandwidth of 0.0157% and a 0.15dB ripple measured under -0.87V control voltage and 16V DC-bias. The device is simply a resonator without an applied control-voltage (V_{DC2}=0) as seen in Fig. 9 (see black curve). Fig. 10 compares the filter performance under different DC-bias, in which the filter bandwidth can be reduced with increasing DC-bias and decreasing control-voltage.

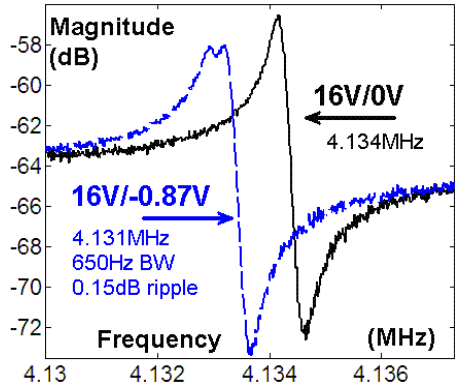

Figure 9. Comparison of resonator and filter performance at different control voltages

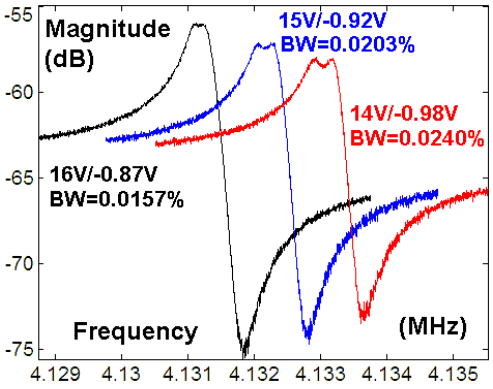

Figure 10. Filter Bandwidth reduction with increasing DC-bias and decreasing control-voltage.

The relation between the optimized control-voltage (output) and the DC-bias (input) is shown in the dotted line in Fig. 9. The plotted curves show the variation in the frequencies of the resonant peaks. The bandwidth (spacing between the curves) decreases with increasing DC-bias and decreasing control-

voltage. In principle, the minimum filter bandwidth is limited by the maximum driving voltage (pull-in) of the device.

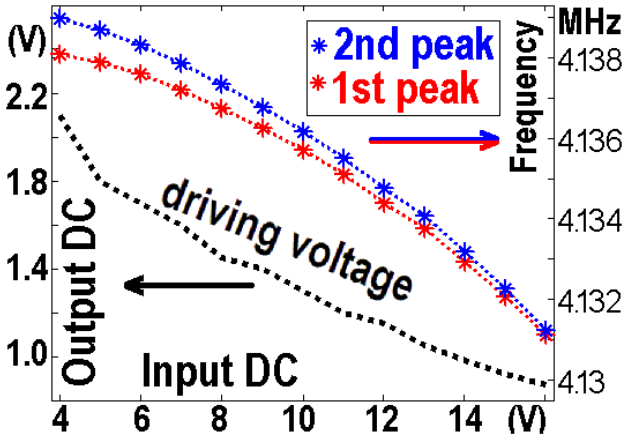

Figure 11. Optimized control-volatge and DC-bias curve of minimum filter bandwidth.

III. Summary of Phase Inversiion Priciple with Different Coupling Mechanisms

A novel MEMS capacitively coupled twin-beam resonator-array filter utilizing an internal phase inverter technique with differential DC bias driving has been demonstrated in a silicon microfabrication process, with a frequency of 4.134MHz, a 3dB-bandwidth of 0.0157% and a 0.15dB ripple measured under -0.87V control-voltage and 16V DC-bias. The filter bandwidth is voltage tunable employing the electrical spring softening effect to an order of magnitude less than a microfabricated mechanical spring.

This technique can be compared with the internal electrical phase inversion [1] and mechanical phase inversion [2] techniques presented earlier, that realize the same function for filter design. Table 1 compares the mechanical and electrical phase inversion mechanisms and summarizes the coupling techniques utilized in this paper and in previous work. Table 2 compares the performance of the resonator arrays and filters described in this paper and previous work [1][2].

The mechanical and internal electrical phase inversion methods integrated with multiple coupling techniques enhances the design flexibility for MEMS resonator based filters and the principle can be extended to filters based on other resonators.

TABLE I. Summary of Phase Inversion Filters

	Phase inversion filter family	
	Phase inversion technique	***Coupling methods***
Lamé filter I [2]	Mechanical inversion	Wire
Lamé filter II [2]	Mechanical inversion	Electrical
DETF Filter [1]	Differential DC-bias	Anchor
Twin-beam filters	Differential DC-bias	Capacitive

TABLE II. Filters Performance Comparison

	Filter Performance Comparison			
	Centre Freq	***Bandwidth***	***Ripple***	***DC-bias***
Lamé filter I [2]	44.4MHz	0.1%	0.1dB	50/50V
Lamé filter II [2]	29.6MHz	0.05%	0.2dB	40/40V
DETF Filter [1]	2.29MHz	0.36%	2.7dB	6/-6.55V
Twin-beam filters	4.13MHz	0.0157%	0.15dB	16/-0.87V

References

[1] J. Yan, A.A. Seshia, K.L. Phan, J.T.M. van Beek, 'Internal Electrical Phase Inversion for FF-beam Resonator Arrays and Tuning Fork Filters', Proc. IEEE Int. Conf. on Micro Electro Mechanical Systems, Tucson, Arizona, USA, pp. 1028-1031, Jan 13-17, 2008

[2] J. Yan, A.A. Seshia, K.L. Phan, J.T.M. van Beek, 'Mechanical Phase Inversion for Coupled Lamé Mode Resonator Array Filters', Proc. IEEE Int. Conf. on Micro Electro Mechanical Systems, Tucson, Arizona, USA, pp. 1024-1027, Jan 13-17, 2008

[3] J. Yan, A.A. Seshia, K.L. Phan, P.G. Steeneken, and J.T.M. van Beek, 'Narrow Bandwidth Single-Resonator MEMS Tuning Fork Filter,' IEEE Int. Frequency Control Symposium, Geneva, Switzerland, pp.1366-1369, May 29 - June 1, 2007.

[4] G.K. Ho, R. Abdolvand, and F. Ayazi, 'Through-support-coupled micromechanical filter array,' Proc. IEEE Int. Conf. on Micro Electro Mechanical Systems, Maastricht, The Netherlands, pp. 769-772, Jan. 25-29, 2004

[5] S. Natsiavas, 'Mode localization and frequency veering in a non-conservative mechanical system with dissimilar components,' J. Sound Vibrat., vol. 165 , pp. 137-147, 1993

[6] S.D. Senturia, 'Microsystem design,' Kluwer Academic Publishers, 2001.

[7] C. T.-C. Nguyen and R. T. Howe, 'An integrated CMOS micromechanical resonator high-Q oscillator,' IEEE J. Solid-State Cir., vol.34, no.4, pp. 440-455, 1999

[8] J.R. Clark, W.-T. Hsu, M.A. Abdelmoneum, and C.T.-C. Nguyen, 'High-Q UHF micromechanical radial-contour mode disk resonators,' J. Microelectromech. vol. 14, no.6, pp. 1298-1310, 2005